JOURNAL OF CHEMICAL INFORMATION AND MODELING

Article

pubs.acs.org/jcim

Searching the "Biologically Relevant"Conformation of Dopamine: A Computational Approach

Sebastian A. Andujar,[†,‡] Rodrigo D. Tosso,[†,‡] Fernando D. Suvire,[†] Emilio Angelina,[§] Nelida Peruchena,[§] Nuria Cabedo,[∥] Diego Cortes,[∥] and Ricardo D. Enriz*[,†,‡]

[†]Departamento de Química, Universidad Nacional de San Luis, Chacabuco 915, 5700 San Luis, Argentina

[‡]IMIBIO-SL (CONICET), Chacabuco 915, 5700 San Luis, Argentina

[§]Laboratorio de Estructura Molecular y Propiedades, Área de Química Física, Departamento de Química, Facultad de Ciencias Exactas y Naturales y Agrimensura, Universidad Nacional del Nordeste, Avda. Libertad 5460, (3400) Corrientes, Argentina

[∥]Departamento de Farmacología, Facultad de Farmacia, Universidad de Valencia, 46100 Burjassot, Valencia, España

Supporting Information

ABSTRACT: We report here an exhaustive and complete conformational study on the conformational potential energy hypersurface (PEHS) of dopamine (DA) interacting with the dopamine D2 receptor (D2−DR). A reduced 3D model for the binding pocket of the human D2−DR was constructed on the basis of the theoretical model structure of bacteriorhodopsin. In our reduced model system, only 13 amino acids were included to perform the quantum mechanics calculations. To obtain the different complexes of DA/D2−DR, we combined semiempirical (PM6), DFT (B3LYP/6-31G(d)), and QTAIM calculations. The molecular flexibility of DA interacting with the D2−DR was evaluated from potential energy surfaces and potential energy curves. A comparative study between the molecular flexibility of DA in the gas phase and at D2−DR was carried out. In addition, several molecular dynamics simulations were carried out to evaluate the molecular flexibility of the different complexes obtained. Our results allow us to postulate the complexes of type A as the "biologically relevant conformations" of DA. In addition, the theoretical calculations reported here suggested that a mechanistic stepwise process takes place for DA in which the protonated nitrogen group (in any conformation) acts as the anchoring portion, and this process is followed by a rapid rearrangement of the conformation allowing the interaction of the catecholic OH groups.

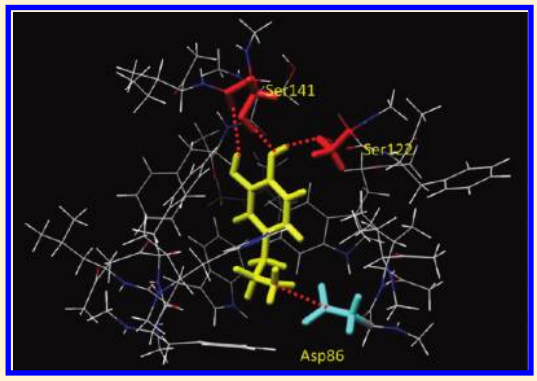

INTRODUCTION

In general, different efforts in medicinal chemistry and neuropharmacology have yielded substantial numbers of compounds with activity and selectivity at each of the major DA (dopamine) receptors.[1−6] However, it is remarkable that few truly innovative chemical entities of new pharmacophoric principles can be identified among recently developed DA receptor-directed compounds.[7] It has also been difficult to design compounds that lack interactions with other monoaminergic receptors, which bear considerable molecular homology to DA receptors. It is clear that the major challenge is to clarify some molecular aspects involved in the DA−receptor interactions. In fact, the design and development of DA receptor-selective ligands remains largely empirical, quite conservative in following molecular precedents, and somewhat unpredictable and not ready for routine applications of computer-aided drug design techniques. The computational limitations and/or errors can arise in many ways, depending on the methodology used. Among other factors, the inadequate sampling of internal degrees of freedom, structure of the complex, and the so-called "ligand-receptor conformational problem" have received relatively little attention in this case, at least in comparison with other aspects. Among the many factors considered as related to the pharmacological activity of a drug, a particularly prominent role is attributed to its conformation. We might think that a good ligand binds in a relatively low energy conformation since its internal energy contributes to the total free energy of binding. However, it has been observed that in the majority of cases the bioactive conformation of a flexible ligand does not correspond to the global energy minimum of the same ligand in its free state, and in many cases it does not even correspond to a local minimum.[8] In fact, a previous analysis of 150 protein−ligand complexes found that the bound conformer is 4−5 kcal/mol higher in energy on average than the lowest-energy conformer in solution.[9] This observation is consistent with the induced fit theory[10−14] according to which both ligand and protein can reorganize themselves in order to adopt the complementary shapes required for binding. Thus, a question that has intrigued generations of chemists is what features of a particular small molecule are responsible for its biological activity. This question is important to some because of its significance in understanding

Received: September 8, 2011
Published: December 7, 2011

dx.doi.org/10.1021/ci2004225 | J. Chem. Inf. Model. 2012, 52, 99−112

biology and to others because it may lead to a better and safer drug. Many types of data and theories may be used to probe this question, but most start with some hypothesis as to the general types of forces that are involved in ligand−receptor interactions.

The ensemble of conformations DA can access is critical to many aspects of drug design, since these conformations define the shape of the molecule, which in turn is a major determinant of its biological properties. Already, few rotameric positions per bond and few alternate ring geometries lead to a large number of theoretically possible conformations that DA could in principle attain. The challenge faced by a medicinal chemist is to understand the structural and energetic differences between these conformations so as to successfully design new molecules that adopt the desired shape with little or no energetic penalty. The conformational properties of DA present us with a four-faced problem, corresponding to the four principal situations in which they are studied: (i) the isolated molecule, (ii) the molecule in the crystal, (iii) the molecule in solution, and (iv) the molecule at the receptor. There have been both experimental and computational investigations of the conformational properties of DA in the past. In the solid state, the aminoethyl side chain is in anti conformer form, and the catechol ring is in a perpendicular arrangement.[15] Solmajer et al.[16] studied the conformational equilibrium for DA in D_2O using H NMR. There are in the literature many conformational studies using different quantum mechanical calculations for DA in the gas phase.[17−20] Our own research group reported the potential energy surface obtained for DA from *ab initio* calculations.[21] With respect to calculations performed considering the solvent effects, the most comprehensive conformational study for protonated DA was probably carried out by Nagy et al.[22] Other previously reported studies have used different approaches.[23,24]

A relatively large number of theoretical conformational studies of DA and related molecules[17−24] have been previously reported. However, these studies have neglected important conformational ingredients. Most contributions using quantum mechanical calculations have attacked the problem of DA−receptor interactions by determining the most probable structure of the isolated drug or in solution, using the methods of physical and theoretical chemistry. However, it seems appropriate to survey first some biological aspects of such interactions, keeping in mind that the conditions of living systems place important restrictions on the applicability of theoretical methods. Taking advantage of structural information available from different experimental and theoretical studies of DA at the D_2 dopamine receptor (D2−DR) structure, we performed a comprehensive conformational study of DA interacting with this D2 receptor, using a combination of molecular dynamics (MD) simulations and semiempirical and DFT calculations. In addition, a detailed electronic analysis using quantum theory of atoms in molecules (QTAIM)[25−27] techniques was carried out for the different complexes obtained.

In principle, there seems to be a large amount of impressive information about the conformational intricacies of DA interacting at D2−DR. However, reality is somewhat different; there is, in fact, only partial information about this old and interesting problem. The questions which arise are as follows: Which is/are the "biologically relevant" conformation/s of DA? How is the molecular flexibility of DA located at the binding site? Is the molecular flexibility large enough to allow conformational interconversions within the receptor?

It has been noted that conformational flexibility may be of importance both for the ligand and for its biological target. DA has been shown to have a significant molecular flexibility (at least in the gas phase and in solution) and because of this the possibility of forming numerous energetically different conformations. This property makes the determination of the biologically active conformation of DA complicated. In order to solve this problem, three basically different approaches have been attempted by various research groups:

(i) First is the determination of the most energetically stable conformation of DA using crystallographic methods (X-ray diffraction studies), nuclear magnetic resonance, and quantum mechanical calculations in the gas phase and solution. Some researchers hypothesize that the energetically most favorable form of DA in solution was also the biologically most active conformation. However, it should be noted that the conformers predominating in solution or in the crystal are not necessarily the conformers predominating in active sites where rotational barriers might be altered as the result of intra- or intermolecular interactions. In addition, serious problems emerge when the solvation state of a ligand as DA binds to a receptor. Methods used for obtaining structural and thermodynamic parameters for a solute molecule surrounded by an abundance of solvent molecules do not apply for a ligand partially solvated (or not solvated) in the depth of a protein. It is clear that DA binding at D2−DR cannot be modeled by a simple interaction of two molecules in solution.

(ii) Second is the synthesis and pharmacological testing of DA analogues with a rigid or semirigid structure. The natural or synthetic compounds showing high activities enable an indirect indication as to the active conformation of DA. However, it is clear that this is an indirect approach.

(iii) The third approach has been the simulation of the DA/D2−DR interactions using MD simulations. There are in the literature many studies reporting MD simulations for both agonists and antagonists of DA using different homologated receptor models.[28,29] However, in comparison to the many MD simulations performed for other ligands, there are very few simulations specifically carried out for DA (the endogenous ligand). Also, these simulations do not deal with the relationships of the local energy minima on the energy hypersurface. In particular, the lowest barriers separating the various conformations have generally been ignored, leading to a poor understanding of the conformational properties of DA at D2−DR. This situation is compounded by an almost exclusive use of very simple force fields in automatic searches with molecular mechanics calculations. Thus, interesting details about the conformational intricacies of DA interacting with D2−DR remain unknown.

The comparison between the conformational behavior of DA in different environments and the degree of similarity between active site conformations and low energy solution structures of the same ligand will provide an indication of the physics of binding. For example, to what extent does the receptor induce structural changes in DA when bound to the active site? Does it substantially deform the solution structure of DA with binding involving "key reshaping" of the ligand as proposed for peptides,[30] or is the change in DA structure negligible, with the lock and key mechanism[31] holding? How "rusty" is the lock and key model for this ligand?

A question which might arise is, why DA? The DA molecule is an appropriate choice for this study not only because of its

important standing in biochemistry but also because it offers an opportunity to study the conformational properties of a flexible ligand which has exhibited a number of different conformations in the gas phase and aqueous solution but whose PEHS can be reasonably approximated by considering only the rotation of a reduced number of dihedral angles.

For the first time, an exhaustive and complete conformational study about the conformational PEHS of DA interacting with D2−DR has been performed using combined semiempirical/*ab initio*/DFT and QTAIM calculations. The ultimate goal of this report might be defined as the search for the "biologically relevant" conformation of DA; this information is expected to help us in designing drugs acting on the receptor. The road of this goal is undoubtedly very arduous, as many different factors play a role in drug action. However, despondence is not an answer to the problem. One has to dissect the problem into simple steps, which are open to theoretical calculations and permit relatively accurate answers. One of these steps is the study of the conformation of DA at D2−DR, which obviously determines its ability to make contact with the receptor site.

METHODS OF CALCULATIONS

Calculations were carried out in three steps. In a first step, we performed a preliminary MD simulation of the molecular interactions between DA and D2−DR (Figure 1). In this figure, we might appreciate a spatial view of DA interacting with DA−RD_2; the binding pocket is also shown. In the second step, reduced model systems were optimized using quantum mechanics calculations. Semiempirical calculations (PM6,[32] MOPAC program[33]) were employed in these optimizations. The most representative complexes obtained in the previous steps were further analyzed from a QTAIM study. Finally, several MD simulations were carried out using as input files the different complexes.

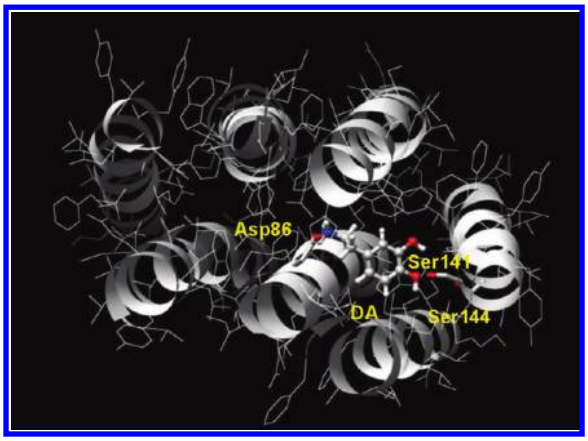

Figure 1. Spatial view of DA interacting with the DA−RD_2 using the Chimera program as a graphic interface. In this figure, the interaction of DA with Asp86 (TM3), Ser141 (TM5), and Ser144 (TM5) is shown.

Molecular Dynamics Simulations. It must be pointed out that the principal goal of the MD simulations performed here is not to obtain a new D2−DR by homology. Our aim in this study is less ambitious; we wish to obtain a reasonable indication about the biologically relevant conformation of DA interacting with the D2−DR. Thus, for such a purpose, we considered it more appropriate to use a previously reported and extensively tested model for D2−DR. In fact, there are many molecular modeling studies in the literature reporting D2−DRs obtained by homology, all of them structurally closely related.[28,29,34−39] Even when some of these models display small structural differences, the majority are very similar and do not show significant differences, at least at the binding pocket zone. In such a situation, we decided to use a previously reported model from which we recently obtained an excellent correlation between our experimental results and the theoretical results,[38−40] indicating that this model is good enough for our purposes.

A 3D model of the human D2−DR was used for the MD simulations, based on the X-ray structure of bacteriorhodopsin[35] (PDB acquisition code: 1I15). The ligand topologies were built using the MKTOP program.[42] For the first MD simulations, we have used an approach where manual docking was guided by information from site-directed mutagenesis and short docking simulations with both the receptor and the ligand free to move. Structurally similar parts of the DA were oriented in similar positions in the receptor model, which was described by Mansour et al.[43] and Lan et al.[37] For the MD simulations performed for the different complexes, the input files were constructed from the geometries obtained with quantum mechanics optimizations.

The MD simulations and analysis are performed using the GROMACS 3.2.1 simulation package[44,45] with the OPLS-AA force field[46−51] and the rigid SPC water model[52,53] in a cubic box with periodic boundary conditions. The receptor−ligand complexes were embedded in a box containing the SPC water model that extended to at least 1 nm between the receptor and the edge of the box, resulting in a box with 7.22 nm side lengths. The total number of water molecules was 11 349 for the different simulations. Then three Na^+ ions were added to the systems by replacing water in random positions, thus making the whole system neutral. The time step for the simulations was 0.002 ps, for a complete simulation time of 5 ns. For long-ranged interactions, the particle-mesh Ewald (PME)[54,55] method was used with a 1 nm cutoff and a Fourier spacing of 0.12 nm. The MD protocol consisted of several preparatory steps: energy minimization using the conjugate gradient model,[56,57] density stabilization (NPT conditions), and finally production of the MD simulation trajectory. All production simulations were performed under NVT conditions at 310 K, using Berendsen's coupling algorithm[58] for keeping the temperature constant. The compressibility was 4.8×10^{-5} bar^{-1}. All coordinates were saved every 5 ps. The SETTLE[45] algorithm was used to keep water molecules rigid. Also, the LINCS[59] algorithm was used to constrain all C-α atom positions for the receptor in order to avoid desfolding problems. The analysis of the simulations was performed using the analysis tools provided in the GROMACS package.

Considering the 5 ns of MD simulation and from the time profiles, it was concluded that some properties (total, potential, and kinetic energies) of the ligand−receptor complexes reached stable average values around 0.5 ns, whereas others took longer periods of time. For such a reason, to ensure full equilibration, only the last 4.5 ns were taken into account for the analysis. After discarding the first 0.5 ns of the trajectory, we followed the changes of spatial ordering of the ligand−receptor complexes.

The DA D2−DR used here is lacking the intra- and extracellular loops connecting the transmembrane helixes. Such loops are proposed to play a role in the recognition of the ligands, as well as in the biofunctionality of the receptor. These loops certainly also play a role in the stabilization of the whole system while immersed in the cellular membrane.

dx.doi.org/10.1021/ci2004225 | J. Chem. Inf. Model. 2012, 52, 99−112

In order to bypass this limitation, we constrained the Cα of the transmembranes helixes during the simulation time. Thus, it must be pointed out that the model used in this work is rather "complex" yet far from complete.

Quantum Mechanics Calculations. A reduced 3D model of the human D2−DR was constructed on the basis of the theoretical model structure of bacteriorhodopsin.[35] The binding pocket of D2−DR was defined according to Teeter et al.[35] and Neve et al.[36] In our reduced model system, only 13 amino acids were included for the molecular simulations. The size of the molecular system simulated and the complexity of the structures under investigation restricted the choice of the quantum mechanical method to be used. Consequently, the semiempirical PM6 method was selected for calculations. The torsional angles of the ligands and the flexible side chains of the amino acids as well as the bond angles and bond lengths of the moieties involved in the potential intermolecular interactions were optimized at the semiempirical level. In contrast, the torsional angles of backbones as well as the bond angles and bond lengths of noninteracting residues were kept frozen during the calculations.

TOPOLOGICAL STUDY OF THE ELECTRON CHARGE DENSITY DISTRIBUTION

Several selected conformations of molecular complexes, obtained from our "reduced model system", were used as input by the calculation of the charge density. Single point calculations were realized with Gaussian 03 employing a hybrid B3LYP functional and 6-31+G(d,p) as a basis set. This type of calculation has been used in recent works on the topology of $\rho_{(r)}$ because it ensures a reasonable compromise between the wave function quality required to obtain reliable values of the derivatives of $\rho_{(r)}$ and the computer power available, due to the extension of the system in study.[60]

The topological properties of a scalar field such as $\rho_{(r)}$ are summarized in terms of their critical points, i.e., the points r_c where $\Delta\rho_{(r)} = 0$. Critical points are classified according to their type (ω,σ) by stating their rank (ω) and signature (σ). The rank is equal to the number of nonzero eigenvalues of the Hessian matrix of $\rho_{(r)}$ at r_c, while the signature is the algebraic sum of the signs of the eigenvalues of this matrix. Critical points of the (3, −1) and (3, +1) types describe saddle points, while the (3, −3) is a maximum and (3, +3) is a minimum in the field. The determination of all of the critical points of the electron charge density distribution, bond paths, calculations of local topological properties of the $\rho_{(r)}$ at the critical point, and the display molecular graphs were performed with the AIM2000 package.[61]

OVERVIEW OF ATOMS IN MOLECULES THEORY

Here, we only present the essential theoretical information that is needed for the understanding of the molecular graphs (networks of bond path in the density topology), in DA/D2−DR complexes, because the use of topological concepts in the description of intra/intermolecular interactions is well documented in the standard literature.[62] The electron charge density, $\rho(r)$, is a physical quantity that has a definite value at each point in space. QTAIM analysis is based on the critical points (CPs) of this electronic density distribution. The gradient vector of the charge density $(\Delta\rho_{(r)})$ vanishes at these points, which are characterized by the three eigenvalues ($\lambda1$, $\lambda2$, and $\lambda3$) of the Hessian matrix of the charge density.

In the topological distribution of the electronic charge density, three topological features or elements appear as a consequence of the interaction between two atoms: (a) a bond critical point (BCP), (b) a bond path (BP), and (c) an interatomic surface (IAS). A BCP has two negative eigenvalues and a positive eigenvalue. The two negative eigenvalues of the Hessian matrix ($\lambda1$ and $\lambda2$) measure the degree of contraction of the charge density at BCP ($\rho(r)$) perpendicular to the bond toward the critical point, while the positive eigenvalue ($\lambda3$) measures the degree of contraction parallel to the bond and from the BCP toward each of the neighboring nuclei. As mentioned above, the eigenvectors associated with the eigenvalue $\lambda3$ define a unique pair of trajectories of $\Delta\rho(r)$ that originate in the (3, −1) BCP, each of which terminates at the nucleus of one of the neighboring atoms (3, −3). This pair of trajectories defines *a line through space along which the electron density is a maximum with respect to any neighboring line* forming an atomic interaction line (AIL) or *bond path*. Each bond path is homeomorphically mirrored by a virial path, a line of maximum negative potential energy density linking the same nuclei. Thus, the presence of a bond path and its associated virial path provides a universal indicator of bonding between the atoms so linked.

Three other critical point types can be defined in the topology of $\rho(r)$: (3,+1) or the ring critical point, RCP; (3, −3) or the nuclear critical point, NCP, associated with the nuclei; and (3,+3) or the cage critical point, CCP. This last CP type appears when several rings topologically describe a cage.

Spatial views shown in Figures 1 and 3−6 were constructed using the UCSF Chimera program[63] as the graphic interface.

RESULTS AND DISCUSSION

Obtaining the Starting Structure for the Complex DA/D2−DR. There are in the literature many studies reporting different simulations of DA, agonists and antagonists interacting with the human D2−DR. All of them describe the DA binding site in the human D2−DR. In addition, point mutation studies give experimental evidence for such a binding site.[35−37,43] Therefore, considering that there is a general agreement about the location and structural characteristics of this binding site, we locate DA in the top third of the seven-transmembrane (7-TM) barrel involving TM domains 3−6 (see Figure 1). The first step of our study was to simulate the molecular interaction of DA with D2−DR, using molecular dynamics calculations in order to obtain a starting structure for the complex DA/D2−DR. Our results are in complete agreement with the previously reported simulations,[34−41] indicating that the following residues are essential for DA binding in the human D2−DR. These residues are as follows: Phe82, Val83, Asp86, and Val87 (TM3); Ser118 and Ser121 (TM4); Ser141, Ser144, and Phe145 (TM5); and Trp182, Phe185, Phe186, and His189 (TM6). However, it must be pointed out that the conformation obtained for DA at the end of this simulation is not necessarily the "biologically relevant" conformation. Can we realistically expect to make accurate and reliable predictions with simulations that are decidedly crude representations of the molecular interactions involved in the binding process? Any model that neglects or else poorly approximates the terms that are playing determinant roles such as lone pair directionality in hydrogen bonds (HBs), explicit π-stacking polarization effects, hydrogen bonding networks, induced fit, and conformational entropy cannot reasonably be expected to determine the molecular interactions stabilizing the

dx.doi.org/10.1021/ci2004225 | J. Chem. Inf. Model. 2012, 52, 99−112

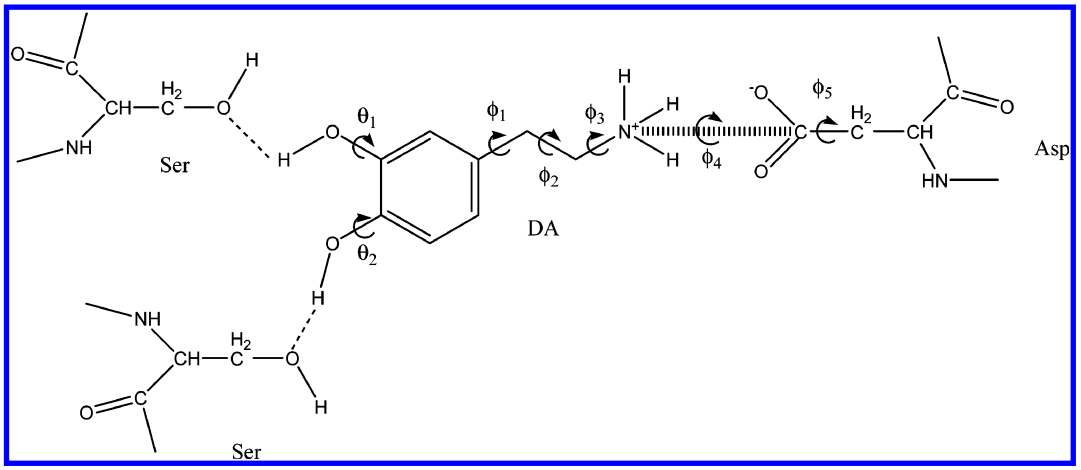

Figure 2. A general scheme of DA at the binding site. The different torsional angles determining the possible spatial orderings of DA in the complex are shown in this scheme.

ligand at the binding site. There are in the literature several works supporting this concept.[64,65] On the basis of such concepts, it is clear that the final conformation obtained for DA from a simple MD simulation is not necessarily the biologically relevant conformation, or at least there is room for reasonable doubts in this respect.

Obtaining the Different DA/D2−DR Complexes. DA has a determined number of conformers in the gas phase and aqueous solution which have been extensively studied.[16−24] Furthermore, it is relatively easy to construct input files for molecular computations for such conformers. However, nobody can make even an educated guess about how many conformers might be associated with DA interacting with D2−DR (the so-called biologically relevant conformers). The problem is even more complex if we are also interested in analyzing the transition state structures and the different interconversion pathways potentially involved in such a process. Thus, information about local and global minima of DA interacting with D2−DR may not be enough. It is better to have at least a good notion of the shape and also some indication about the molecular flexibility of the small ligand in the binding pocket. A comprehensive computational method to answer the above questions might be to find out how the different conformations are linked together, and this requires an exploration of a larger part of the multidimensional PEHS of DA linked to D2−DR. Thus, a full understanding of conformational space requires identification of a more complete network of conformational interconversions of DA at D2−DR. In principle, the overall conformational behavior of DA at D2−DR looks like a complex conformational problem with seven torsional angles (ϕ_1−ϕ_5, θ_1, and θ_2; Figure 2). The overall orientation of DA with respect to the binding pocket is described by the dihedral angles ϕ_4 and ϕ_5. The orientation of the two hydroxyl groups of the catechol ring are described by the dihedral angles θ_1 and θ_2, whereas the orientations of the flexible side chain (interacting with Asp86) are mainly determined by the torsional angles ϕ_1−ϕ_5.

Considering that ϕ_5 determines the general spatial position of DA at the binding site, the first step in our conformational analysis was to determine the energetically preferred orientations for this dihedral. Thus, we calculated the PEC for ϕ_5 using PM6 calculations. On the basis of the topological periodicity of ϕ_1, the multidimensional conformational analysis (MDCA)[66−68] predicted four different spatial positions for this angle. However, our PM6 calculations predicted only three spatial orderings for this angle ($\phi_5 \approx -120°$, $\phi_5 \approx 120°$, and $\phi_5 \approx -60°$). The missing conformation ($\phi_5 \approx 60°$) is a consequence of steric hindrances with the binding pocket. From this result, we considered only these three positions as starting geometries in our conformational analysis. Thus, we performed a systematic conformational study of DA evaluating the other six torsional angles (ϕ_2− ϕ_5, θ_1, and θ_2). More than 130 different DA/D2−DR complexes were obtained from this analysis. However, we have included in Table 1 only those complexes possessing values less than 37 kcal/mol above the global minimum. We selected this energy window on the basis of previously reported discussions about this topic. An important problem is how much above the global energy minimum we must go in a conformational search in order to be reasonably sure to have included the bioactive conformation.[69] Various estimates of the upper conformational energy limit to be used in a search for a bioactive conformation have been given in the literature. In the context of pharmacophore identification, Marshall and Motoc[70] observed that a reasonable estimation varied in the range of 5−20 kcal/mol. Siebel and Kollman[71] found it reasonable to expect that the bioactive conformations for highly active molecules had conformational energy penalties of less than 4−5 kcal/mol. Liljefors and Pettereson[69] advocated the use of an upper conformational energy limit of 2.5−3 kcal/mol. Thus, we considered that 35 kcal/mol is a very reasonable energy window in this case.

Table 1 shows different values obtained for the torsional angles ϕ_1−ϕ_5 in these complexes. The catechol ring, which is determined by ϕ_1, adopts values from −126° to 124°, whereas this ring for DA in the gas phase displays only values near −90° and 90°. For ϕ_2, DA in the gas phase displays three highly preferred conformations (60°, 180°, and −60°). However, for the different DA/D2−DR complexes obtained, this angle adopts values from −174° to −59° as well as from 49° to 179°.

Ligand flexibility in the active site prompts us to define similarity in broad terms. In this paper, we considered two metrics of similarity: the first, based on the value of the torsion angles, considering the relative position of a subset of atoms and the second, regarding the potential stabilizing molecular interactions. Thus, on the basis of the different spatial orderings adopted by DA and its receptor, as well as the different intermolecular interactions observed, we clusterized the 46 complexes in five different types (**A**−**E**, Table 1). A common

dx.doi.org/10.1021/ci2004225 | J. Chem. Inf. Model. 2012, 52, 99−112

Table 1. Different Types of DA−DR_2 Complexes Showing the Torsional Angles and Energy Gaps[a]

complex conformation	ϕ_1 (deg)	ϕ_2 (deg)	ϕ_3 (deg)	ϕ_4 (deg)	ϕ_5 (deg)	ΔE (kcal/mol)	type
1	−110.70	−77.78	−64.72	141.46	−137.23	0.00	**A**
2	−118.00	−105.00	−18.70	79.30	−137.23	1.54	**A**
3	−55.30	−81.10	−107.80	172.50	−137.23	3.60	**A**
4	84.40	56.42	43.53	83.43	120.00	3.83	**B**
5	89.80	−81.8	−21.20	81.30	−137.20	4.11	**A**
6	81.79	58.80	38.74	87.67	118.56	4.16	**B**
7	−56.40	−74.53	149.72	−135.16	−60.00	4.18	**A**
8	82.88	65.85	61.59	56.82	120.00	4.19	**B**
9	100.35	73.93	73.37	−116.42	−60.00	4.53	**A**
10	84.20	88.59	1.56	89.54	−60.00	4.78	**A**
11	87.38	61.39	65.75	55.24	120.00	5.12	**B**
12	81.99	65.61	61.37	175.54	120.00	5.15	**B**
13	69.30	179.21	−136.76	23.15	−137.23	5.26	**A**
14	−68.26	−170.54	−30.30	122.11	−60.11	6.27	**A**
15	118.36	−74.09	110.60	79.69	−59.75	6.47	**A**
16	−126.72	−101.77	81.30	112.78	120.00	6.49	**A**
17	39.05	49.11	94.65	−129.38	−60.00	6.51	**B**
18	−61.58	169.55	0.24	−63.95	−60.00	6.58	**A**
19	−121.90	−107.70	128.39	−11.34	−60.00	6.76	**A**
20	−68.54	−59.83	173.21	−123.20	−60.00	6.79	**B**
21	88.39	78.04	55.11	−124.02	−60.00	7.02	**A**
22	−35.59	−174.41	94.68	1.22	−130.00	7.74	**A**
23	72.67	167.60	−5.80	−63.10	−60.00	7.78	**A**
24	124.59	−169.07	119.16	4.25	−137.23	8.00	**A**
25	61.00	170.10	−14.20	−57.60	−60.00	8.58	**A**
26	57.65	−109.28	76.90	107.15	−59.84	8.66	**B**
27	83.64	−92.04	28.31	−179.81	−62.39	8.93	**A**
28	−52.60	134.96	10.59	−88.73	−60.00	9.36	**B**
29	−90.49	49.30	99.82	−91.15	118.93	9.39	**B**
30	76.67	111.94	−69.36	−41.29	−60.00	10.06	**A**
31	−124.72	177.78	−111.75	−65.04	−60.00	11.02	**C**
32	−7.03	170.90	−22.70	−55.50	−60.00	11.04	**A**
33	19.20	−158.59	24.92	−47.52	−60.00	11.36	**A**
34	−34.98	−174.41	104.23	−75.62	−60.00	11.73	**A**
35	39.95	−73.45	−90.00	65.35	−60.00	11.90	**D**
36	−52.16	−89.39	27.30	0.36	−60.20	11.97	**A**
37	91.60	−64.40	−26.10	−95.60	−137.20	12.53	**E**
38	−60.50	176.70	−39.04	−52.10	−60.00	12.66	**A**
39	94.91	173.57	−146.56	−75.23	−137.23	13.62	**A**
40	−110.50	−109.80	−2.50	−9.90	−60.00	13.68	**A**
41	−83.41	87.94	32.29	−119.85	−60.00	14.20	**A**
42	29.90	−89.64	−74.00	62.70	−60.00	16.17	**D**
43	−30.00	−84.08	−124.15	−169.82	120.00	20.29	**E**
44	−56.40	−74.83	173.21	−123.20	−60.00	25.40	**A**
45	22.09	155.20	133.89	111.68	−137.23	28.30	**B**
46	76.54	58.87	71.48	47.51	120.00	34.79	**A**

[a]The torsional angles θ_1 and θ_2 determining the spatial ordering of both catecholic hydroxyl groups were not included in this table for simplicity.

characteristic displayed for all of the complexes obtained here is a strong interaction between the protonated amino group of DA and Asp86. However, the different complexes displayed spatial orderings which are characteristic of each type. The complexes of type **A** are the most populous (30 complexes), and the principal characteristic is that they adopt an adequate conformation to allow interactions between the OH groups of the catechol ring with a cluster of serines formed by Ser141, Ser144, and Ser122. Thus, these complexes displayed stabilizing hydrogen bonds (HB) between the OH groups (*p* or *m* position) and the different serines. The global minimum belongs to this type of complex, and a spatial view of such a conformation is shown in Figure 3. It is interesting to note that this complex is stabilized by strong intermolecular interactions. They are a salt bridge between the protonated nitrogen of DA and Asp86 (0.29 nm of distance) and a hydrogen bond of the catecholic *m*-OH group with the carbonyl group of Ser141 (0.31 nm of distance). In addition, the catecholic *p*-OH group displays a bifurcated hydrogen bond with Ser141 and Ser122 showing distances of 0.22 and 0.19 nm, respectively.

Another interesting complex of type **A** is complex **13** (Figure S1, Supporting Information) in which DA adopts a conformation very similar to that reported for the crystal.[15] This complex displayed a value 5.26 kcal/mol above the global

dx.doi.org/10.1021/ci2004225 | J. Chem. Inf. Model. 2012, 52, 99−112

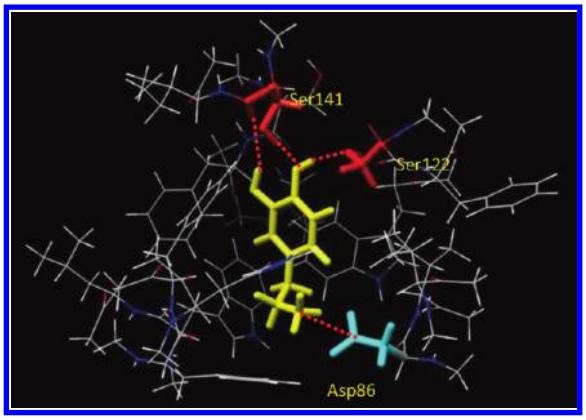

Figure 3. Spatial view of complex **1** (global minimum) in the binding pocket. Water molecules were deleted in this reduced model in order to better appreciate the stabilizing interactions of the complex.

minimum, and the principal stabilizing interactions are the following: a hydrogen bond between the catecholic *m*-OH group with the carbonyl group of the peptide bond of Ser141 and interactions with two aromatic amino acids Phe145 (TM5) and Phe185 (TM6). Complexes of type **A** possess very different energies; for example, the energy gap between complex **1** and complex **46** (Figure S3, Supporting Information) is 34.7 kcal/mol. Between both complexes, there are 28 other different complexes of type **A** possessing different energies. There are three factors which could explain the different energies observed for these complexes.

(a) The first one is the different type of HB observed between the catecholic OH groups and Ser141. The stronger the interaction is, the greater the stabilization. Among the different HBs we observed are bifurcated interactions, interactions with the OH group in the *meta* position, with the OH group located in the *para* position, with the OH group of Ser141, with the CO group of Ser141, with the catecholic OH acting as a donor and with the catecholic OH acting as an acceptor. Our results indicated that the catecholic OH acting as a proton donor gives stronger interactions in comparison when this group acts as a proton acceptor.

(b) A second factor modifying the stability of the complex is the steric hindrance with Asp86. Some complexes displayed the oxygen atoms of Asp86 eclipsed by the hydrogen of the side chain, which enhanced the energy of the system.

(c) A third factor is the spatial ordering of Phe185. The side chain of this amino acid possesses a significant molecular flexibility, and therefore, an adequate spatial ordering allows an optimal interaction minimizing the steric hindrance.

Figure 4 gives a spatial view for the different complexes of type **A** obtained in Table 1.

Complexes of type **B** do not present interactions with the cluster of serines; instead, they interact with hydrophobic amino acids (Phe145, Phe186, and Trp182) located in the vicinity of the serine residues. There are 11 complexes of type **B** in the selected energy window. The different energies observed in these complexes might be due, at least in part, to the different steric hindrance observed for the ligand in these complexes.

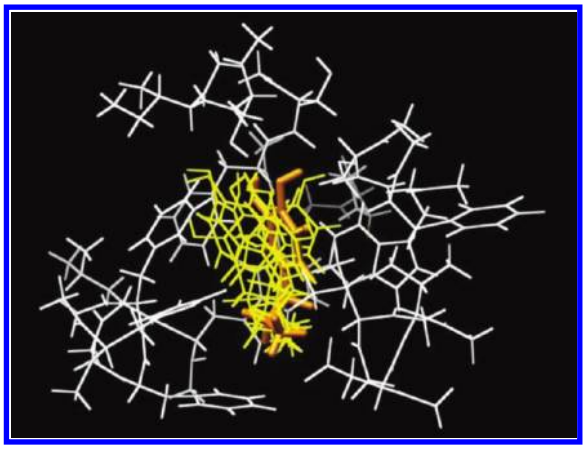

Figure 4. Superimposed spatial view of the different conformers obtained for DA (type **A**) where the global minimum is denoted in orange. The structure of the receptor was kept fixed in the spatial ordering obtained for the preferred complex for simplification.

Figure S2 (Supporting Information) shows a spatial view of complex **4**. The interactions between DA with Phe145 (TM5), Phe185 (TM6), and Trp182 (TM6) might be well appreciated in this figure.

Spatial views for the 11 complexes of type **B** are shown in Figure 5.

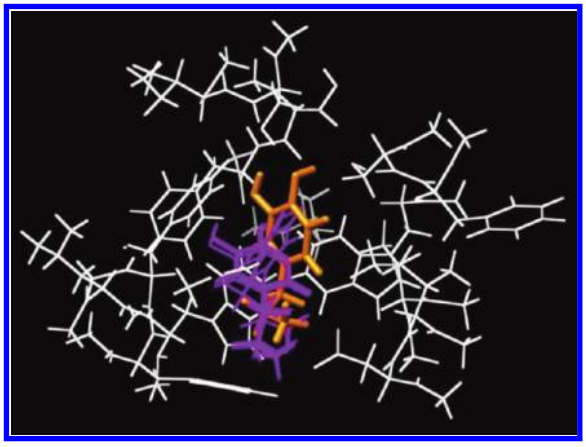

Figure 5. Superimposed spatial view of the different conformers obtained for DA (type **B** in purple) where the global minimum is denoted in orange. The structure of the receptor was kept fixed in the spatial ordering obtained for the preferred complex for simplification.

There is only one complex of type **C** considering this energy window. This is complex **31** in Table 1, which displays an energy gap of 11.02 kcal/mol. This complex presents a stabilizing interaction between the catecholic OH group in the *meta* position with the nitrogen atom of His189. There are two complexes of type **D** (complexes **35** and **42**) characterized by an interaction between the aromatic ring of DA with Trp182. Complexes of type **E** (**37** and **43**) in turn display a spatial ordering in which DA is practically located out of the binding site. Figure 6 gives a comparative spatial view for complexes **C**, **D**, and **E**. The different spatial orderings adopted by DA in these complexes might be appreciated in this figure.

At this stage of our work, it is possible to obtain a general schematic representation of D2−DR which describes the different complexes obtained (Figure 7). Thus, in complexes of type **A**, DA once joined to Asp86 might interact with a polar

dx.doi.org/10.1021/ci2004225 | *J. Chem. Inf. Model.* 2012, 52, 99−112

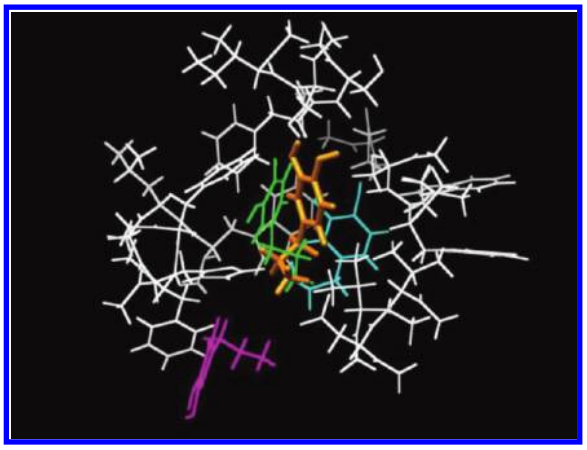

Figure 6. Superimposed spatial view of the different conformers obtained for DA (type **C** in green, type **D** in light blue, and type **E** in fuchsia). In this figure, the global minimum is denoted in orange, and the structure of the receptor was kept fixed in the spatial ordering obtained for the preferred complex for simplification.

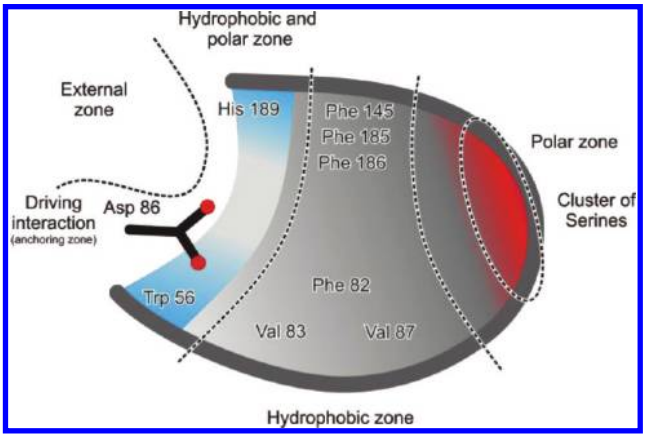

Figure 7. Schematic view of the binding site of DA showing the different binding zones (hydrophobic and polar) and the amino acids involved.

region where the serines cluster is located. In contrast, in complexes of type **B**, DA is stabilizing the molecular system interacting with the aromatic residues (Phe145, Phe186, and Trp182) located in the adjacent hydrophobic region. In the case of complexes of types **C** and **D**, DA could interact with the so-called polar and hydrophobic region, giving alternative interactions with His189 and Trp182, respectively. Complexes of type **E** display a completely different conformational behavior, locating the catecholic ring in an external region of the binding site.

Evaluating the Molecular Interactions in the Binding Pocket. The topological analysis of the electron density constitutes a powerful tool for investigating the electronic properties of the molecular system and allows for a deep examination of the molecular interactions. This methodology has been successfully applied in the study of the properties of a variety of conventional and unconventional HBs, aromatic HBs, and $\pi-\pi$ stacking.[25−27]

From the QTAIM, it is possible to determine in an unequivocal way the different strong and weak interactions between two atoms observing the existence of bond critical points (BCPs) and their respective bond paths. It should be noted that this detailed analysis is not possible from the evaluation of the geometrical parameters (bond distances and angles).

On the basis of our QTAIM study, two groups of complexes were obtained: (i) complexes in which the catecholic OH groups are making HBs with Ser141 and Ser144 (complex type A: **1**−**3**, **5**, **7**, **9**, and **10**) and (ii) complexes where the catecholic OH groups are interacting with no polar residues of the binding pocket (complex type **B**: **4**, **6**, **8** and **11**; type **C**: **31**; and type **D**: **42**).

Figure 8 shows the molecular graph obtained for conformation **1** of DA interacting at the binding site. In this

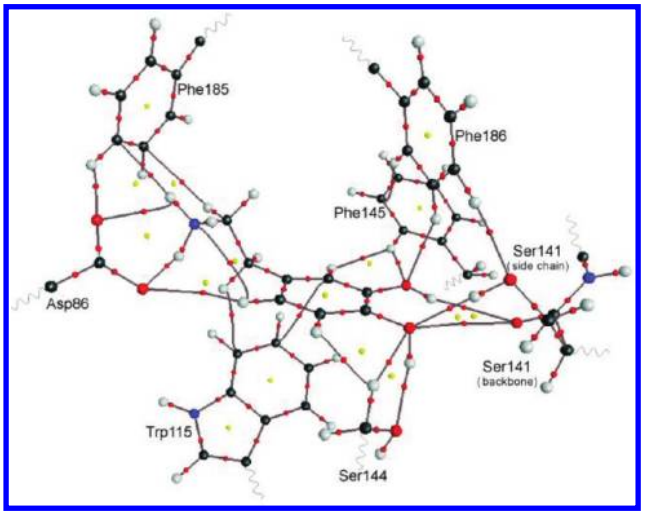

Figure 8. Molecular graph obtained for the conformation of DA (complex **1**) interacting at the binding site. The net of interactions involving different regions of the DA molecule can be observed in this figure. Big circles correspond to attractors or the nuclear critical point (3, −3), attributed to nuclei. Lines connecting the nuclei are the bond paths, and the small red circles on them are the bond critical points or (3, −1) critical points. The small yellow circles are ring critical points or (3,+1) critical points.

figure, the net of interactions involving different regions of the DA molecule can be observed. In Figure S4, Supporting Information, only the HBs involving the catecholic OH with Ser141 and Ser144 were plotted, to better appreciate such interactions.

In conformation **1**, the *p*-OH is acting as a proton donor, and the OH group of Ser144 is the proton-aceptor counterpart. However, the *p*-O is acting as an acceptor of both the OH group of Ser141 and the H−C_β of the side chain of Ser144. In addition, a BCP between the *p*-O and the C═O group of the backbone of Ser141 (*p*-O···O_{Ser141}) was obtained. This latter interaction was observed only for complexes **1** and **3**. The *m*-OH makes an HB with the C═O group of the Ser141 backbone, whereas *m*-O is acting as a proton-acceptor of two weak HB interactions (type O···H−C) with the aromatic rings of Phe145 and Phe186 (see Figures 8 and S4).

Figure 9 gives the electronic density (ρ_b) located in the BCP for the different interactions obtained for the catecholic HO groups of complexes of type **A** (**1**−**3**, **5**, **7**, **9**, and **10**). This figure shows that complex **1**/D2−DR displayed the highest number of interactions for the catecholic OH groups (seven interactions). For complex **2**, the catecholic *m*-OH displayed exactly the same interactions as the *m*-OH of complex **1**

dx.doi.org/10.1021/ci2004225 | J. Chem. Inf. Model. 2012, 52, 99−112

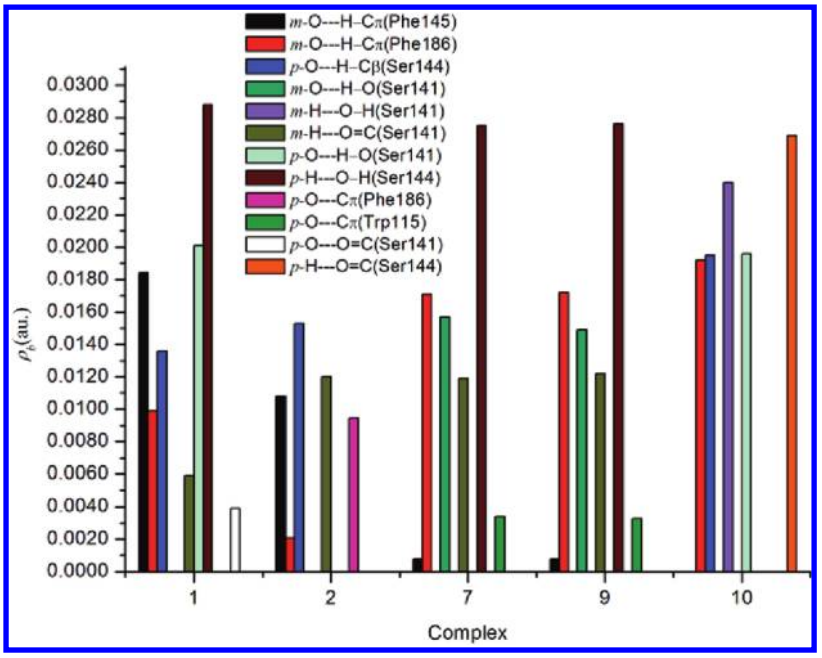

Figure 9. Electronic density (ρ_b) located in the BCP for the different interactions obtained for the catecholic HO groups of the different complexes of type **A** evaluated from QTAIM analysis.

(*m*-O···H−C(Phe145), *m*-O···H−C_π(Phe186), and *m*-OH···O═C(Ser141)), but the *p*-OH presents only two interactions (*p*-O···C_π(Phe186) and *p*-O···H−C_β(Ser141)).

Figure S5, Supporting Information, shows the molecular graphs obtained for complex **7**. In complexes **7** and **9**, the *p*-H makes a HB *p*-OH···O(Ser144), whereas the *p*-O is interacting with Trp115 throughout a weak interaction *p*-O···C_π(Trp115). The *m*-OH, in turn, makes two HBs with Ser141 (*m*-H interacts with the C═O of the backbone and *m*-O is accepting the proton from the OH group). This group is also acting as a proton-aceptor of two weak HB interactions O−H···C_π with the aromatic rings of Phe145 and Phe186 (Figure S5).

In complex **10**, the *p*-H makes a HB with the C═O of the Ser144 backbone, and *p*-O is acting as a proton-acceptor from the HO of Ser141 and H−C_β of Ser144. In addition, the *m*-H makes HBs with the OH of the side chain of Ser141. The *m*-O is making two nonconventional HBs of the type O···H−C_π with two H−C_π bonds from the aromatic ring of Phe186 (Figure S6, Supporting Information).

Evaluating the Conformational Flexibility of DA at the Active Site. Further research has to be carried out to study the rotational barriers of DA, as well as the dependence of these barriers on the environment in which the molecule is located. Thus, in order to better understand the molecular flexibility displayed by DA at D2−DR, we calculated several potential energy surfaces (PESs) scanning ϕ_1 versus ϕ_2. We chose these torsional angles for two reasons: (a) because both angles determine the conformation of DA and (b) because it is possible to compare these PESs with those previously reported in the gas phase. We evaluated 10 different PESs, those being the two surfaces shown in Figure 10, representatives of the overall phenomena. These surfaces are rather complicated compared to that of the gas phase. Most noticeable is the fact that the symmetry of gauche-perpendicular regions has become totally distorted. This is not unexpected considering the asymmetry of the environment. Figure 10a shows the PES where the global minimum is located (complex **1**, signaled with a star in this figure). PM6 calculations predicted that the conformational interconversion between the conformation of DA obtained in complex **1** (global minimum) and the conformation of DA obtained in complex **5** required about 7.5 kcal/mol. Figure 10b shows that the energy requirement necessary to connect the different zones possessing low-energy is also about 7.5 kcal/mol.

On the other hand, comparing Figure 10a and b, it is clear that the molecular flexibility obtained for DA at the active receptor site is markedly more restricted than that obtained in the gas phase. This is particularly evident after observing the general shapes obtained for these PESs. Surfaces shown in Figure 10a and b are very intricate, displaying deep valleys with gentle slopes. This conformational restriction observed for the torsional angles ϕ_1 and ϕ_2 is a consequence of the steric hindrance between DA and the neighboring amino acids.

To further compare the conformational behavior of DA at the receptor and in isolation, we included in Figure 11 the different conformers obtained for DA in the 46 complexes shown in Table 1. It is interesting to note that in general the conformations obtained for DA in the different complexes might be grouped in the energetically preferred zones of the PES attained in the gas phase. Although some conformations are located in energetically nonpreferred zones, it is also true that they are not located in the zone of the maximum or zones possessing very high energy. In other words, we can conclude that the conformational behavior obtained for torsional angles ϕ_1 and ϕ_2 at the bioactive site in general is not too different from that obtained for the isolated molecule. However, it is also clear that the molecular flexibility observed for DA in both environments is very different.

On the basis of these results, in the next step of our study, we decided to evaluate the molecular flexibility of DA at the receptor site from potential energy curves (PECs). The interconversions among the different complexes **A**, **B**, **C**, **D**, and **E** were evaluated by scanning the geometrical distance between the oxygen atom of Ser141 and the oxygen atoms of

dx.doi.org/10.1021/ci2004225 | J. Chem. Inf. Model. 2012, 52, 99−112

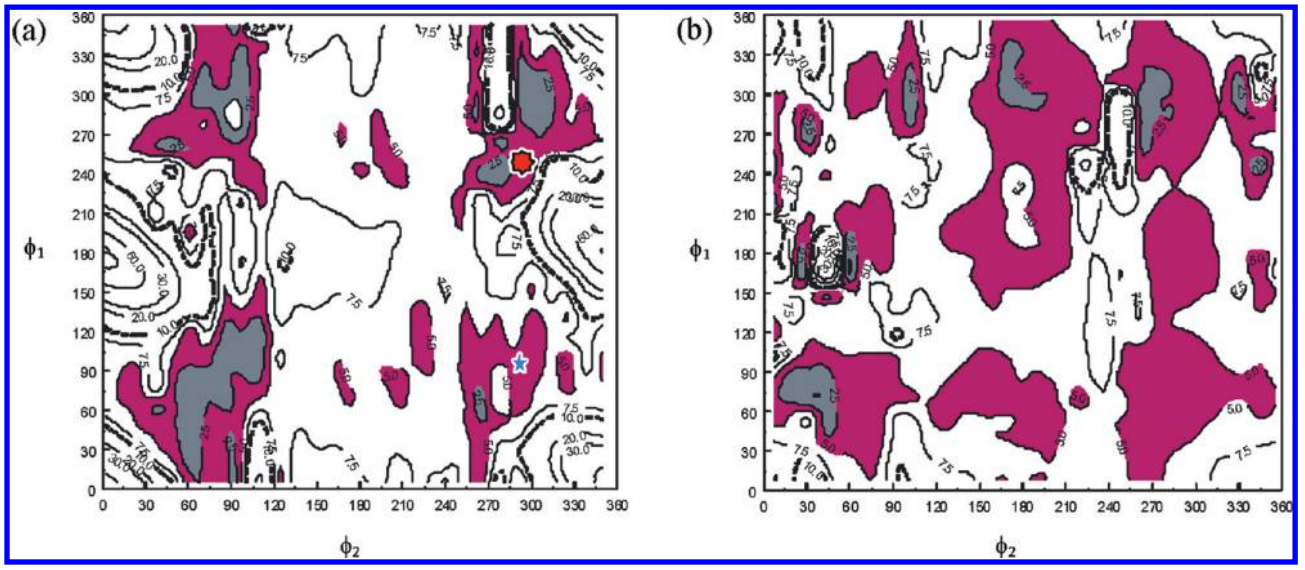

Figure 10. Potential energy surface obtained for DA at the binding site scanning ϕ_1 vs ϕ_2. The surfaces were obtained from PM6 calculations. All of the torsional angles were optimized using the following starting values for the rest of the torsional angles: (a) $\phi_3 \approx -64°$, $\phi_4 \approx 141°$, and $\phi_5 \approx -137$. (b) $\phi_3 \approx -146°$, $\phi_4 \approx -91°$, and $\phi_5 \approx 120$.

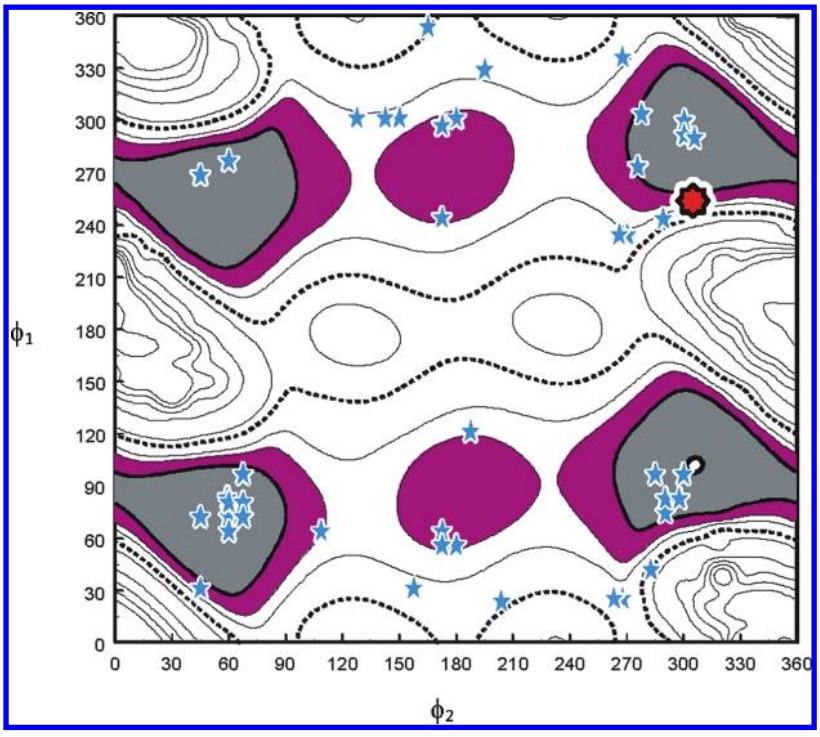

Figure 11. Potential energy surface obtained for DA in the gas phase. The conformations adopted by DA in the different complexes are denoted with stars, whereas the conformation adopted in complex **1** (global minimum) is denoted with a red star.

both catecholic hydroxyls. Thus, the starting points for each PEC corresponded to the interatomic distances between the catecholic hydroxyls and the oxygen atom of Ser141 obtained for the different complexes (**B**, **C**, **D**, and **E**), whereas the end points corresponded to the distance obtained for the catecholic hydroxyls and the oxygen atom of Ser141 for the nearest **A** complex.

Figure 12a shows the interconversion process between complex **4** (type **B**) and complexes **2** and **1** (both type **A**). This change required only 0.5 kcal/mol, indicating that complexes of type **B** might be poorly stable and the conformational interconversion between forms **B** and **A** can occur without a significant energetic requirement.

Figure 12b shows the interconversion between complex **35** (**D**) and complexes **6** (type **B**) and **1** (type **A**). In this case, the interconversion requires about 7.5 kcal/mol, which is higher with respect to the previously described interconversion. Figure 12c, in turn, shows the interconversion process between complex **37** (type **E**) and complex **11** (type **B**) through complex **35** (type **D**). This interconversion requires about 2 kcal/mol, and this curve suggests that complex **E** has the lowest stability among these complexes. It is interesting to note that

dx.doi.org/10.1021/ci2004225 | J. Chem. Inf. Model. 2012, 52, 99−112

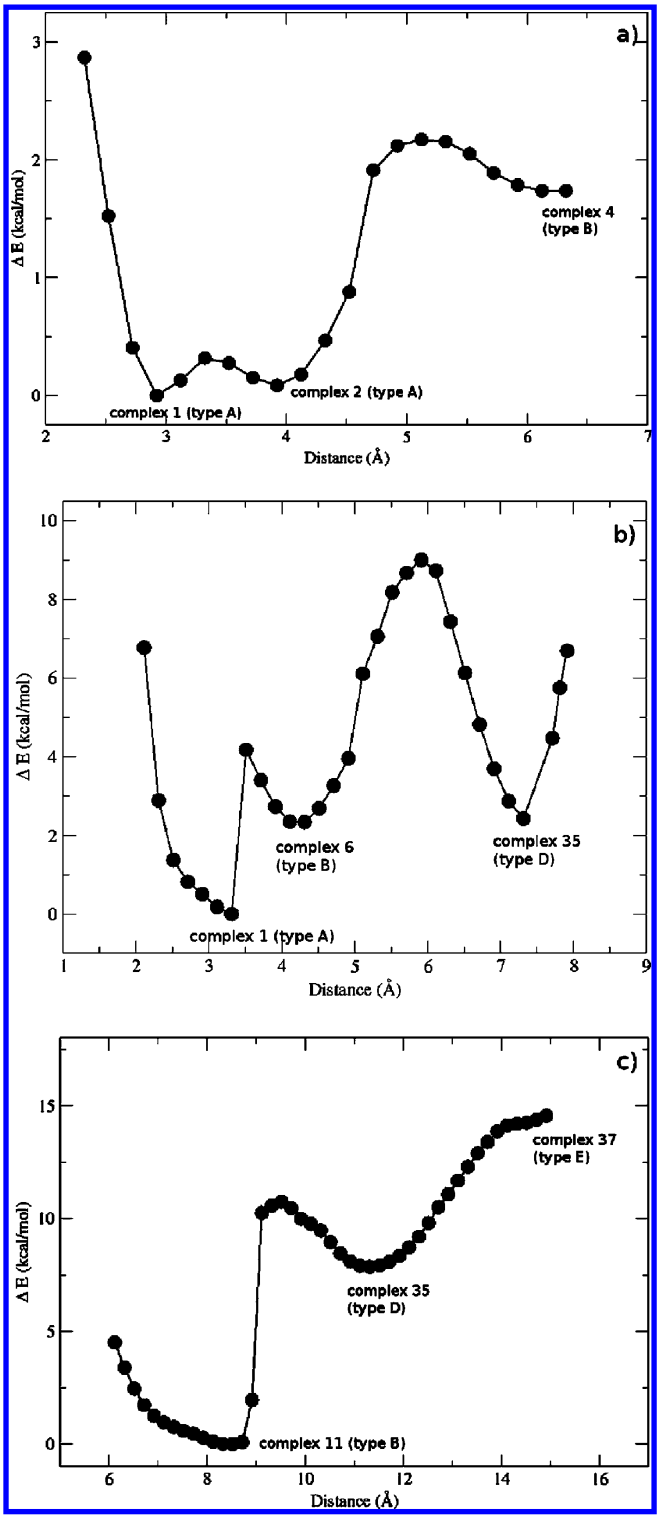

Figure 12. Potential energy curves showing the interconversions among the different complexes **A**, **B**, **C**, **D**, and **E**. Interconversions were evaluated by scanning the geometrical distance between the oxygen atom of Ser141 and the oxygen atoms of both catecholic hydroxyls. (a) Interconversion between complexes **A** and **B**. (b) Interconversion among complexes **D**, **B**, and **A**. (c) Interconversion among complexes **E**, **B**, and **A**.

this curve gives additional information about the stabilizing interactions on DA when the molecule is moving from the external moiety of the binding pocket to its internal zone. The favorable gradient observed in this interconversion might explain, at least in part, the tendency of DA to form the low-energy complexes of type **A**.

Finally, in the last step of our study, we performed several MD simulations starting from the different types of complexes obtained (**B**, **C**, **D**, and **E**) in order to determine if DA is maintained in these forms or if, on the contrary, it converges to the energetically preferred complex type **A**. Thus, two simulations of 5 ns for the different complexes were carried out. All of the simulations give as the final form one of the energetically preferred **A** complexes. However, it must be pointed out that different starting points are necessary to obtain the different preferred complexes of type **A**. From these results, we can conclude that by performing several MD simulations using the adequate starting points, it is possible to obtain the most relevant conformational information, that is, to determine the energetically preferred complexes. However, it is also true that interesting information about the conformational intricacies and spatial hindrance at the binding pocket is missing when using only standard MD simulations. Our exploratory analysis of the HSEPC of DA interacting with the human D2−DR allows one to obtain interesting interactions which have not been previously described (at least in detail). The stabilizing interactions between the catecholic ring and the hydrophobic residues Phe185, Trp182, and His189 illustrate this situation very well. It is interesting to note that such interactions might be very important for the design of new antagonists for D2−DR.

Determining the Mechanism for the Binding Process. Considering the moderate but significant molecular flexibility obtained for DA at the active site, it is not easy to determine which conformations might be biologically relevant for this molecule. However, on the basis of our theoretical results, it appears that the preferred **A** type forms, and a rapid interconversion between them might be necessary to produce the biological response.

The conformational selection of the flexible DA binding to the active site of the D2−DR can have different procedures. Thus, the mechanism of the binding process can presume two general cases: (a) at any instant, only those DA molecules having the appropriate single conformation are able to bind to the receptor. Each portion of DA binds simultaneously to the appropriate subsite of the binding site. This model is associated with the idea that the preferred conformation in solution is relevant for binding. However, in this case, there is not an *a priori* reason why this should be so. Also, there are a number of instances in which the conformation of a ligand bound to a protein has shown to be different from the preferred conformation in solution. (b) Another possibility is that binding takes place by a stepwise process in which the protonated nitrogen group (in any conformation) acts as the anchoring portion, making a strong salt bridge with Asp86, and this process is followed by a rapid rearrangement of the conformation DA so as to permit the interaction of the remaining functional moiety (the catecholic OH groups). An important difference between these models is that, in the second case, the actual conformational distribution of DA is less crucial, while the rate at which conformational interconversions can occur becomes considerably significant. Accepting the validity of the PM6 calculations and MD simulations reported here, it seems that model 2 or an intermediate model sharing aspects of both models (1 and 2) is more probable for DA. A range of conformations for the side chain linking the protonated portion and the OH groups seems to be well

dx.doi.org/10.1021/ci2004225 | J. Chem. Inf. Model. 2012, 52, 99−112

tolerated to produce the biological response. However, it is clear that no conformation may be operative. A high-energy barrier might force the molecule to bind by the "all-or-none" mechanism (model 1) rather than by the zipper mechanism (model 2). Our calculations predict that barriers of about 7.5 kcal/mol are separating the different conformations, and therefore, the conformational interconversions are somewhat restricted but still available for DA. Also, a large part of the conformationally available space is accessible within a low value of energy with respect to the global minimum. Note that MD simulations predict that DA is visiting the different forms predicted by the semiempirical calculations. This is an additional support for model 2 or at least an intermediate model.

It should be noted that we kept the Cα atoms constrained to generate the reduced models which would not allow relaxation of the transmembrane helixes after ligand binding, which may affect the conformational freedom of the ligand in the pocket of the active site. Therefore, some caution is needed with respect to the mechanims proposed here.

CONCLUSIONS

In summary, from our results, two important conclusions might be obtained. The first one is about the "biologically relevant conformation" of DA; the second one is related to the importance of evaluating the conformational behavior of a ligand inserted in the active site considering the entire biological environment.

The conformation of DA is clearly relevant to any consideration of its interaction with the receptor. DA is flexible and, thus, may exist at the receptor in a number of conformations in equilibrium. If one assumes, as seems highly probable, that DA has only a limited number of conformations in its complex with the receptor, then the formation of this complex must involve a process of "conformational selection" which will influence the kinetics and energetics of complex formation. On the basis of our results, it appears that the energetically preferred complexes of type **A** would be the "biologically relevant conformations of DA" to interact with D2−DR. In addition, the theoretical calculations reported here suggested that a mechanistic stepwise process takes place for DA in which the protonated nitrogen group (in any conformation) acts as the anchoring portion, and this process is followed by a rapid rearrangement of the conformation, allowing the interaction of the catecholic OH groups.

Bohem and Klebe reported that for polar ligands in particular, a single crystal structure of a ligand alone is not a reliable predictor of the bioactive conformation.[72] Rather than relying on a single structure, more robust results can be attained when considering multiple structures which sample a variety of local environments. Our results obtained for DA are an additional support for such premises. It should be noted that in a multicomponent biological process, one may be dealing with essentially unidirectional assemblies, each component of which may be triggered from high energy to a low energy conformation following initial ligand attachment. Thus, extrapolating from the conformation of the ligand in the gas phase, in solution or in the crystal to the conformation of the ligand interacting with its receptor, might be a very dangerous approach due to the number of different environmental players involved in such a process which are not satisfactorily considered.

In this paper, we reported our results obtained determining the conformational intricacies of DA interacting with D2−DR. It is expected that this information will lead us a step forward toward the understanding of the biologically relevant conformation of DA, the ultimate goal of the work of many. Although there is still room for some reasonable doubts in some cases, we believe that our results could help in the understanding of the conformational behavior of DA at D2−DR and can serve as a guide for the design of new ligands for this receptor.

ASSOCIATED CONTENT

Supporting Information

Three extra figures displaying spatial views of complexes **13**, **4**, and **46** are given in Figures S1, S2 and S3, respectively. Figures S4, S5, and S6 show molecular graphs obtained for the conformation of DA (complexes **1**, **7**, and **10**). This material is available free of charge via the Internet at http://pubs.acs.org

AUTHOR INFORMATION

Corresponding Author

*Phone: (54) 2652 423789. E-mail: denriz@unsl.edu.ar.

ACKNOWLEDGMENTS

Grants from Universidad Nacional de San Luis (UNSL) partially supported this work. This research was also supported by the Spanish "Ministerio de Educación y Ciencia" grant SAF 2007-63142. S.A.A. is thankful for a postdoctoral fellowship from CONICET—Argentina. E.A. is a fellow researcher at CONICET—Argentina. R.D.E and N.P are members of the Consejo Nacional de Investigaciones Científicas y Técnicas (CONICET—Argentina) staff.

REFERENCES

(1) Bettinetti, L.; Löber, S.; Hübner, H.; Gmeiner, P. Parallel synthesis and biological screening of dopamine receptor ligands taking advantage of a click chemistry based BAL linker. *J. Comb. Chem.* **2005**, *7*, 309−316.

(2) Kebabian, J. W.; Tarazi, F. I.; Kula, N. S.; Baldessarini, R. J. Compounds selective for dopamine receptor subtypes. *Drug Discovery Today* **1997**, *2*, 333−340.

(3) Baldessarini, R. J. Dopamine receptors and clinical medicine. In *The Dopamine Receptors*; Neve, K. A., Neve, R. L., Eds.; Humana Press: Totowa, NJ, 1997; pp 457−498.

(4) Mailman, R. B.; Nichols, D. E.; Tropsha, A. Molecular drug design for dopamine receptors. In *The Dopamine Receptors*; Neve, K. A., Neve, R. L., Eds.; Humana Press: Totowa, NJ, 1997; pp 105−133.

(5) Kelleher, J. P.; Centorrino, F.; Albert, M. J.; Baldessarini, R. J. Advances in atypical antipsychotics for the treatment of schizophrenia: New formulations and new agents. *CNS Drugs* **2002**, *16*, 249−261.

(6) Rowley, M.; Bristow, L. J.; Hutson, P. H. Current and novel approaches to the drug treatment of schizophrenia. *J. Med. Chem.* **2001**, *44*, 477−501.

(7) Zhang, A.; Neumeyer, J.; Baldessarini, R. Recent Progress in Development of Dopamine Receptor Subtype-Selective Agents: Potential Therapeutics for Neurological and Psychiatric Disorders. *Chem. Rev.* **2007**, *107*, 274−302.

(8) Jorgensen, W. L.; Maxwell, D.; Tirado-Rives, J. Development and Testing of the OPLS All-Atom Force Field on Conformational Energetics and Properties of Organic Liquids. *J. Am. Chem. Soc.* **1996**, *118*, 11225−11236.

(9) Perola, E.; Charifson, P. Conformational Analysis of Drug-Like Molecules Bound to Proteins: An Extensive Study of Ligand Reorganization upon Binding. *J. Med. Chem.* **2004**, *47*, 2499−2510.

(10) Koshland, D. E. Application of a Theory of Enzyme Specificity to Protein Synthesis. *Proc. Natl. Acad. Sci. U.S.A.* **1958**, *44*, 98−104.
(11) Thoma, J. A.; Koshland, D. E. Competitive Inhibition by Substrate During Enzyme Action Evidence for the Induced-Fit Theory. *J. Am. Chem. Soc.* **1960**, *82*, 3329−3333.
(12) Koshland, D. E. Correlation of Structure and Function in Enzyme Action. *Science* **1963**, *142*, 1533−1541.
(13) Koshland, D. E. Jr. Conformation Changes at the Active Site During Enzyme Action. *Fed. Proc.* **1964**, *23*, 719−726.
(14) Yankeelov, J. A. Jr.; Koshland, D. E. Jr. Evidence for Conformation Changes Induced by Substrates of Phosphoglucomutase. *J. Biol. Chem.* **1965**, *240*, 1593−1602.
(15) Bergin, C. *Acta Crystallogr.* **1968**.
(16) Solmajer, P.; Kocjan, D.; Solmajer, T. Conformational study of catecholamines in solution. *Z. Naturforsch.* **1983**, *38c*, 758−762.
(17) Pullman, B.; Coubiels, J. L.; Courriere, P.; Gervois, J. P. Quantum mechanical study of the conformational properties of phenethylamines of biochemical and medicinal interest. *J. Med. Chem.* **1972**, *15*, 17−23.
(18) Kier, L. B.; Truitt, E. B. Jr. The preferred conformation of dopamine from molecular orbital theory. *J. Pharmacol. Exp. Ther.* **1970**, *174*, 94−98.
(19) Feeney, J.; Roberts, G.; Brown, J.; Burgen, A.; Gregory, H. Conformational study of some component peptides of pentagastrin. *J. Chem. Soc. Perkin Trans. II* **1972**, 601−604.
(20) Urban, J.; Cramer, C.; Famini, G. A computational study of solvent effects on the conformation of dopamine. *J. Am. Chem. Soc.* **1992**, *114*, 8226−8231.
(21) Suvire, F. D.; Cabedo, N.; Chagraoui, A.; Zamora, M. A.; Cortes, D.; Enriz, R. D. Molecular recognition and binding mechanism of N-alkyl-benzyltetrahydroisoquinolines to the D1 dopamine receptor. A computational approach. *THEOCHEM* **2003**, *666−667*, 455−467.
(22) Nagy, P.; Alagona, G.; Ghio, C. Theoretical Studies on the Conformation of Protonated Dopamine in the Gas Phase and in Aqueous Solution. *J. Am. Chem. Soc.* **1999**, *121*, 4804−4815.
(23) Alagona, G.; Ghio, C. The effect of intramolecular H-bonds on the aqueous solution continuum description of the N-protonated form of dopamine. *Chem. Phys.* **1996**, *204*, 239−249.
(24) Urban, J. J.; Cronin, C. W.; Roberts, R. R.; Famini, G. R. Conformational preferences of 2-phenethylamines. A computational study of substituent and solvent effects on the intramolecular amine-aryl interactions in charged and neutral 2-phenethylamines. *J. Am. Chem. Soc.* **1997**, *119*, 12292−12299.
(25) Koch, U.; Popelier, P. L. A. Characterization of C-H...O Hydrogen Bonds on the Basis of the Charge Density. *J. Phys. Chem.* **1995**, *99*, 9747−9754.
(26) Matta, C. F.; Castillo, N.; Boyd, R. J. Extended Weak Bonding Interactions in DNA: π-Stacking (Base−Base), Base−Backbone, and Backbone−Backbone Interactions. *J. Phys. Chem. B* **2005**, *110*, 563−578.
(27) Mosquera, R. A.; Moa, M. J. G.; Estévez, L.; Mandado, M.; Graña, A. M. An Electron Density-Based Approach to the Origin of Stacking Interactions. In *Quantum Biochemistry*; Matta, C. F., Ed.; WILEY-VCH Verlag GmbH & Co. KGaA: Weinheim, Germany, 2010; Chapter 11.
(28) Kalani, M.; Vaidehi, N.; Hall, S.; Trabanino, R.; Freddolino, P.; Kalani, M.; Floriano, W.; Kam, V.; Goddard, W. III. The predicted 3D structure of the human D2 dopamine receptor and the binding site and binding affinities for agonists and antagonists. *Proc. Natl. Acad. Sci. U.S.A.* **2004**, *101*, 3815−3820.
(29) Becker, O.; Marantz, Y.; Shacham, S.; Inbal, B.; Heifetz, A.; Kalid, O.; Bar-Haim, S.; Warshaviak, D.; Fichman, M.; Noiman, S. Protein-coupled receptors: in silico drug discovery in 3D. *Proc. Natl. Acad. Sci. U.S.A.* **2004**, *101*, 11304−11309.
(30) *INSIGHT II*, version 95.0; Molecular Simulations Inc.: San Diego, CA, 1995.
(31) Gundertofte, K.; Liljefors, T.; Norrby, P.; Pettersson, I. A comparison of conformational energies calculated by several molecular mechanics methods. *J. Comput. Chem.* **1996**, *17*, 429−449.
(32) Stewart, J. J. P. *MOPAC2009*; Stewart Computational Chemistry: Colorado Springs, CO, 2008. http://OpenMOPAC.net (accessed Dec. 2011).
(33) Stewart, J. J. P. Optimization of Parameters for Semiempirical Methods V: Modification of NDDO Approximations and Application to 70 Elements. *J. Mol. Modeling* **2007**, *13*, 1173−1213.
(34) Micheli, F.; Bonanomi, G.; Blaney, F.; Braggio, S.; Capelli, A.; Checchia, A.; Curcuruto, O.; Damiani, F.; Di Fabio, R.; Donati, D.; Gentile, G.; Gribble, A.; Hamprecht, D.; Tedesco, G.; Terreni, S.; Tarsi, L.; Lightfoot, A.; Stemp, G.; MacDonald, G.; Smith, A; Pecoraro, M.; Petrone, M.; Perini, O.; Piner, J.; Rossi, T.; Worby, A.; Pilla, M.; Valerio, E.; Griffante, C.; Mugnaini, M.; Wood, M.; Scott, C.; Andreoli, M.; Lacroix, L.; Schwarz, A.; Gozzi, A.; Bifone, A.; Ashby, C. Jr.; Hagan, J.; Heidbreder, C. 124-Triazol-3-yl-thiopropyl-tetrahydro-benzazepines: a series of potent and selective dopamine D3 receptor antagonists. *J. Med. Chem.* **2007**, *50*, 5076−5089.
(35) Teeter, M. M.; Froimowitz, M. F.; Stec, B.; Durand, C. J. Homology modeling of the dopamine D2 receptor and its testing by docking of agonists and tricyclic antagonists. *J. Med. Chem.* **1994**, *37*, 2874−2888.
(36) Neve, K. A.; Cumbay, M. G.; Thompson, K. R.; Yang, R.; Buck, D. C.; Watts, V. J.; Durand, C. J.; Teeter, M. M. Modeling and mutational analysis of a putative sodium-binding pocket on the dopamine D2 receptor. *Mol. Pharmacol.* **2001**, *60*, 373−381.
(37) Lan, H.; DuRand, C. J.; Teeter, M. M.; Neve, K. A. Structural Determinants of Pharmacological Specificity Between D_1 and D_2 Dopamine Receptors. *Mol. Pharmacol.* **2006**, *69*, 185−194.
(38) Andujar, S. A.; Miglioli de Angel, B.; Charris, J. E.; Israel, A.; Suarez-Roca, H.; Lopez, S. E.; Garrido, M. R.; Cabrera, E. V.; Visbal, G.; Rosales, C.; Suvire, F. D.; Enriz, R. D.; Angel-Guio, J. E. *Bioorg. Med. Chem.* **2008**, *16*, 3233−3244.
(39) Andujar, S.; Suvire, F.; Berenguer, I.; Cabedo, N.; Marín, P.; Moreno, L.; Ivorra, M.; Cortes, D.; Enriz, R. Tetrahydroisoquinolines acting as dopaminergic ligands. A molecular modeling study using MD simulations and QM calculations. *J. Mol. Model.* **2011**. Article in Press. DOI: 10.1007/s00894-011-1061-0.
(40) Berenguer, I.; El Aouad, N.; Andujar, S.; Romero, V.; Suvire, F.; Freret, T.; Bermejo, A.; Ivorra, M.; Enriz, R.; Boulouard, M.; Cabedo, N.; Cortes, D. Tetrahydroisoquinolines as dopaminergic ligands: 1-butyl-7-chloro-6-hydroxy-tetrahydroisoquinoline, a new compound with antidepressant-like activity in mice. *Bioorg. Med. Chem.* **2009**, *17*, 4968−4980.
(41) Wang, Y. T.; Su, Z.-Y.; Hsieh, C.-H.; Chen, C.-L. Predictions of binding for dopamine D2 receptor antagonists by the SIE method. *J. Chem. Inf. Model.* **2009**, *49*, 2369−2375.
(42) Ribeiro, A.; Horta, B.; de Alencastro, R. MKTOP: a program for automatic construction of molecular topologies. *J. Braz. Chem. Soc.* **2008**, *19*, 1433−1435.
(43) Mansour, A.; Meng, F.; Meador-Woodruff, J.; Taylor, L.; Civelli, O.; Akil, H. *Eur. J. Pharm-Mol. Pharmacol. Sect.* **1992**, *227*, 205−214.
(44) Berendsen, H.; Van der Spoel, D.; Van Drunen, R. GROMACS: a message-passing parallel molecular dynamics implementations. *Comput. Phys. Commun.* **1995**, *91*, 43−56.
(45) Lindahl, E.; Hess, B.; van der Spoel, D. GROMACS 3.0: a package for molecular simulations and trajectory analysis. *J. Mol. Model.* **2001**, *7*, 306−317.
(46) van Buuren, A.; Marrink, S.; Berendsen, H. A molecular dynamics study of the decane/water interface. *J. Phys. Chem.* **1993**, *36*, 9206−9212.
(47) Mark, A.; van Helden, S.; Smith, P.; Janssen, L.; van Gunsteren, W. Convergence properties of free energy calculations. A-cyclodextrin complexes as a case study. *J. Am. Chem. Soc.* **1994**, *116*, 6293−6302.
(48) Jorgensen, W.; Chandrasekhar, J.; Madura, J.; Impey, R.; Klein, M. Comparison of simple potential functions for simulating liquid water. *J. Chem. Phys.* **1983**, *79*, 926−935.
(49) van Buuren, A.; Berendsen, H. Molecular dynamics simulation of the stability of a 22 residue alpha-helix in water and 30% trifluoroethanol. *Biopolymers* **1993**, *33*, 1159−1166.

(50) Liu, H.; Muller-Plathe, F.; van Gunsteren, W. A force field for liquid dimethyl sulfoxide and physical properties of liquid dimethyl sulfoxide calculated using molecular dynamics simulation. *J. Am. Chem. Soc.* **1995**, *117*, 4363−4366.
(51) Miyamoto, S.; Kollman, P. SETTLE—an analytical version of the SHAKE and RATTLE algorithm for rigid water models. *J. Comput. Chem.* **1992**, *13*, 952−962.
(52) Berendsen, H.; Postma, H.; van Gunsteren, W.; Hermans, W. Interaction models for water in relation to protein hydration. In *Intermolecular Forces*; Pullman, B., Ed.; Reidel: Dordrecht, The Netherlands, 1981; pp 331−342.
(53) Darden, T.; York, D.; Pedersen, L. Particle mesh Ewald—an N.log(n) method for Ewald sums in large systems. *J. Chem. Phys.* **1993**, *98*, 10089−10092.
(54) Essmann, U.; Perera, L.; Berkowitz, M.; Darden, T.; Lee, H.; Pedersen, L. A smooth particle mesh Ewald method. *J. Chem. Phys.* **1995**, *103*, 8577−8593.
(55) Luty, B.; Tironi, I.; van Gunsteren, W. Lattice−sum methods for calculating electrostatic interactions in molecular simulations. *J. Chem. Phys.* **1995**, *103*, 3014−3021.
(56) Zimmerman, K. All purpose molecular mechanics simulator and energy minimizer. *J. Comput. Chem.* **1991**, *12*, 310−319.
(57) Ferguson, D. Parameterization and evaluation of a flexible water model. *J. Comput. Chem.* **1995**, *16*, 501−511.
(58) Berendsen, H.; Postma, J.; DiNola, A.; Haak, J. Molecular dynamics with coupling to an external bath. *J. Chem. Phys.* **1984**, *81*, 3684−3690.
(59) Hess, B.; Bekker, H.; Berendsen, H.; Fraaije, J. E.M. LINCS: a linear constraint solver for molecular simulations. *J. Comput. Chem.* **1997**, *18*, 1463−1472.
(60) Matta, C. F.; Boyd, R. J. *The Quantum Theory of Atoms in Molecules: From Solid State to DNA and Drug Design*; Wiley-VCH: Weinheim, Germany, 2007.
(61) Blieger-König, F.; Schönbohn, J. *AIM2000 Program Package*; version 2.0; Chemical adviser by R.F.W. Bader, Buöro fur Innovative Software Streibel Biegler-König: Germany, 2002.
(62) Bader, R. F. W. *Atoms in Molecules: A Quantum Theory*; Oxford University Press: Oxford, U.K., 1994.
(63) Pettersen, E.; Goddard, T.; Huang, C.; Couch, G.; Greenblatt, D.; Meng, E.; Ferrin, T. UCSF Chimera—a visualization system for exploratory research and analysis. *J. Comput. Chem.* **2004**, *25*, 1605−1612.
(64) Page, C. S.; Bates, P. A. Can MM-PBSA calculations Predict the specificities of protein kinase inhibitors? *J. Comput. Chem.* **2008**, *27*, 1990−2007.
(65) Mertz, K. M. Limits of free energy computation for protein-ligan interactions. *J. Chem. Theory Comput.* **2010**, *6*, 1769−1776.
(66) Csizmadia, I. General and Theoretical Aspects of the Thiol Group. In *The Chemistry of the Thiol Group*; Patai, S., Ed.; John Wiley and Sons: New York, 1974; Chapter 1, pp 1 −109.
(67) Peterson, M.; Csizmadia, I. Analysis of the topological features of the conformational hypersurface of n-butane. *J. Am. Chem. Soc.* **1978**, *100*, 6911−6916.
(68) Peterson, M.; Csizmadia, I. In *Progress of theoretical organic chemistry*; Csizmadia, I., Ed.; Elsevier: Amsterdam, 1982; Vol. 3, pp 190−266.
(69) Liljefors, T.; Pettersson, I. In *A Textbook of Drug Design and Development*; Krogsgaard-Larsen, P., Liljefors, T., Madsen, U., Eds.; Overseas Publishers Association: Amsterdam, 1996; pp 60−93.
(70) Marshall, G. R.; Motoc, I. In *Molecular Graphics and Drug Design*; Burgen, A. S. V., Roberts, G. C. K., Tute, M. S., Eds.; Elsevier: New York, 1986; pp 115−156.
(71) Siebel, G. L.; Kollman, P. A. In *Comprehensive Medicinal Chemistry*; Hansch, C., Sammes, P. G., Taylor, B., Ramsden, C. A., Eds.; Pergamon: New York, 1990; Vol. 4, pp 125−138.
(72) Boehm, H.-J.; Klebe, G. What can we learn from molecular recognition in protein−ligand complexes for the design of new drugs? *Angew. Chem., Int. Ed.* **1996**, *35*, 2588−2614.